

## THE ADAPTIVE IMMERSSED INTERFACE FINITE ELEMENT METHOD FOR ELASTICITY INTERFACE PROBLEMS\*

Yanzhen Chang

*Department of Mathematics, Beijing University of Chemical Technology, Beijing 100029, China  
Email: changyz@mail.buct.edu.cn*

### Abstract

In this paper, we propose adaptive finite element methods with error control for solving elasticity problems with discontinuous coefficients. The meshes in the methods do not need to fit the interfaces. We establish a residual-based a posteriori error estimate which is  $\lambda$ -independent multiplicative constants; the Lamé constant  $\lambda$  steers the incompressibility. The error estimators are then implemented and tested with promising numerical results which will show the competitive behavior of the adaptive algorithm.

*Mathematics subject classification:* 49J20, 65N30.

*Key words:* Adaptive finite element method, Elasticity interface problems.

### 1. Introduction

The interface problems which involve partial differential equations having discontinuous coefficients across certain interfaces are often encountered in fluid dynamics, electromagnetics, and materials science. Especially, the elasticity problems of multiple phase elastic materials separated by phase interfaces often arise in materials science. Two important examples of such problems occur in the microstructural evolution of precipitates in an elastic matrix due to the diffusion of concentration and in the morphological instability due to stress-driven surface diffusion in solid thin films, cf. e.g., [1–3] and the references therein. The understanding of these physical processes is crucial to improve material stability properties, and in turn to develop new and advanced materials that have many applications in automobile manufacture, aircraft industries, and modern communication technologies.

However, solving such elasticity problems are often very difficult due to complicated geometries, multiple components that appear in these problems. Moreover, the low global regularity and the irregular geometry of the interface, the standard numerical methods which are efficient for smooth solutions usually lead to loss in accuracy across the interface. For these reasons, there has been a great interest recently, in materials science, scientific computing, and applied mathematics communities, in developing efficient and accurate numerical techniques for elasticity problems with interfaces.

In this paper, we propose the elasticity problems with interfaces in which the physical parameters are discontinuous across an interface. Let  $\Omega$  be a bounded domain in  $R^3$  which is divided into two subdomains  $\Omega_1, \Omega_2$  by some surface  $\Gamma = \bar{\Omega}_1 \cap \bar{\Omega}_2$ . The problem we will consider

---

\* Received September 14, 2011 / Revised version received February 1, 2012 / Accepted March 28, 2012 /  
Published online November 16, 2012 /

is the following

$$-\nabla \cdot \sigma(\mathbf{u}) = \mathbf{f} \quad \text{in } \Omega_1 \cup \Omega_2, \quad (1.1)$$

$$[\mathbf{u}]_\Gamma = 0, \quad (1.2)$$

$$[\sigma(\mathbf{u})\mathbf{n}]_\Gamma = 0, \quad (1.3)$$

$$\mathbf{u} = 0 \quad \text{on } \Gamma_D, \quad (1.4)$$

$$\sigma(\mathbf{u})\mathbf{n} = \mathbf{g} \quad \text{on } \Gamma_N. \quad (1.5)$$

Here  $\sigma(\mathbf{u})$  is the stress tensor,  $\mathbf{f} \in L^2(\Omega)^3$  is the given body force and  $\mathbf{g} \in L^2(\Gamma_N)^3$  is the surface load.  $\mathbf{u}$  is the displacement field,  $[\mathbf{v}]_\Gamma$  stands for the jump of a quantity  $\mathbf{v}$  across the interface  $\Gamma$  and  $\mathbf{n}$  denotes the unit outer normal to the boundary of one subdomain, say  $\partial\Omega_1$ . The Lipschitz boundary  $\partial\Omega$  consists of a Neumann part  $\Gamma_N$  with positive surface measure and a Dirichlet part  $\Gamma_D$ .

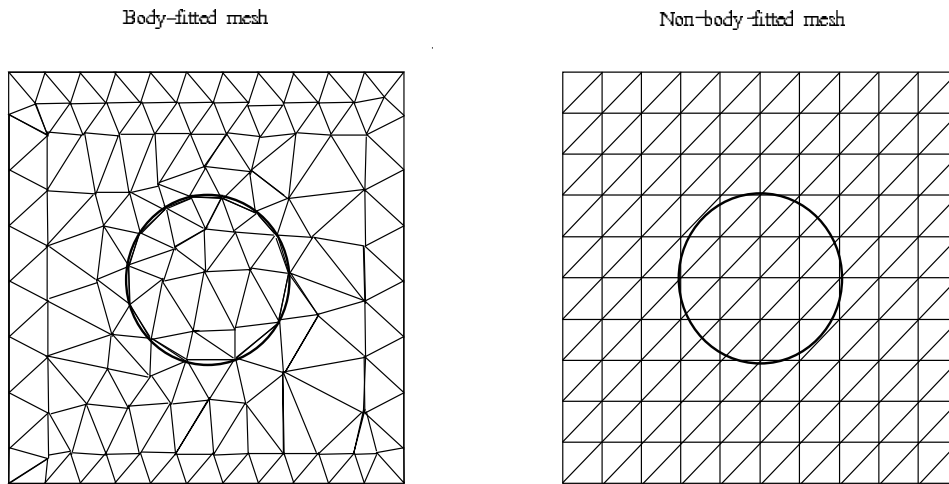


Fig. 1.1. The body-fitted and non-body-fitted mesh in 2D.

We assume that the material is isotropic. So, the stress-strain relation is given by

$$\sigma(\mathbf{u}) = 2\mu\varepsilon(\mathbf{u}) + \lambda \text{tr}(\varepsilon(\mathbf{u}))I,$$

where  $\varepsilon(\mathbf{u}) = \frac{1}{2}(\nabla\mathbf{u} + \nabla\mathbf{u}^T)$  is the linear strain and  $I$  is the  $3 \times 3$  identity matrix.

$$\mu = \frac{E}{2(1+\nu)} \quad \text{and} \quad \lambda = \frac{E\nu}{(1+\nu)(1-2\nu)} \quad (1.6)$$

are the Lamé coefficients,  $E$  is Young's modulus, and  $\nu$  is Poisson's ratio.  $\nu$  is dimensionless and typically ranges from 0.2 to 0.49, and is around 0.3 for most materials. So  $\mu$  and  $\lambda$  are positive and across the interface  $\Gamma$  they are discontinuous. For simplicity, we assume that  $\mu = \mu_i$  and  $\lambda = \lambda_i$  in  $\Omega_i$  for positive constants  $\mu_i, \lambda_i, i = 1, 2$ .

For elliptic interface problems, it is known that optimal or nearly optimal convergence rate can be achieved if body-fitted finite element meshes are used, see e.g. [4, 5]. In a body-fitted mesh, the sides (2D) or the edges (3D) intersect with the interface only through the vertices, see Fig. 1.1. Unfortunately, it is usually a nontrivial and time-consuming task to construct good

body-fitted meshes for problems involving geometrically complicated interfaces. Therefore, numerous modified finite difference methods based only on simple Cartesian grids have been proposed in the literature. We refer to the immersed boundary method in Peskin [14], the immersed interface method in LeVeque and Li [7], Li and Ito [8], the ghost fluid method in Liu et al. [13], and the references therein. In Li et al. [9], an immersed interface finite element method is developed by a local modification of finite element basis functions. As to elasticity interface problems, in Yang [17] and Gong [19], immersed interface method include both FE and FEM are given.

While most of the aforementioned methods assume that the underlying solutions are smooth in each subdomain, they are not easily applied to problems involving non-smooth interfaces. Numerical solutions to this class of problems are challenging in science and engineering applications. It is well-known that the regularity of the solution for interface problems strongly depends on the geometry of the interface and discontinuity of the coefficients in the equation. For interface problems, an exact solution can have strong singularity, so it is essential to develop an adaptive immersed interface finite element method (AIIFEM). In [21], the AIIFEM is developed for solving elliptic and Maxwell interface problems with singularity. They introduce new finite element basis functions for the elements having nonempty intersection with the interface and obtain an AIIFEM which is quasi-optimal in the sense that the energy error decays as  $CN^{-\frac{1}{3}}$ , where  $N$  is the number of degrees of freedom. Motivated by [21], we deal with our elasticity interface problems using the AIIFEM.

In this paper we assume the interface can be of arbitrary shape and the finite element mesh whose vertices are not necessarily located on the interface. The layout of this paper is as follows. In Section 2, we give some precise notations. In Section 3, we derive the a posteriori error analysis and efficient adaptive strategy is proposed. In Section 4, numerical examples are given to support the theoretical results.

## 2. Finite Element Approximation

Let  $\Omega$  be a polyhedral domain in  $R^3$ . For each integer  $m \geq 0$  and real  $p$  with  $a \leq p \leq \infty$ ;  $W^{m,p}$  denotes the standard Sobolev space of real scalar functions with their weak derivatives of order up to  $m$  in the Lebesgue space  $L^p$ . When  $p = 2$ , we use  $H^m$  to stand for  $W^{m,2}$ . Let  $H_D^1 = \{v \in H^1, v|_{\Gamma_D} = 0\}$ .

The weak formulation of (1.1)-(1.5) is to find  $\mathbf{u} \in H_D^1(\Omega)^3$  such that

$$(\sigma(\mathbf{u}), \varepsilon(\mathbf{v})) = (\mathbf{f}, \mathbf{v}) + (\mathbf{g}, \mathbf{v})_{\Gamma_N} \quad \forall \mathbf{v} \in H_D^1(\Omega)^3. \quad (2.1)$$

Let  $\mathcal{M}_h$  be a regular tetrahedral partition of the domain  $\Omega$ . We call an element  $K \in \mathcal{M}_h$  an interface element if the interface passes through the interior of  $K$ ; otherwise we call  $K$  a non-interface element. The set of all interface elements is denoted by  $\mathcal{M}_h^*$ . We assume that for any  $K$  the edge  $e \subset K$  either belongs to  $\Gamma_D$  or  $e \cap \Gamma_D$  has vanishing surface measure, so there is no change of boundary conditions within one edge  $e \in \partial\Omega$ . For any element  $K \in \mathcal{M}_h^*$ , the set of all elements that have nonempty intersection with the interface, we distinguish four cases of how  $\Gamma$  intersects with  $K$ :

- (i) All four vertices lie in one of the two subdomains (Fig. 2.1 (left)).
- (ii) Three vertices A1; A2; A3 lie in one subdomain, the fourth vertex A4 lies in the other subdomain, and  $\Gamma$  intersects each edge A1A4; A2A4; A3A4 at only one point (Fig. 2.1 (right)).

(iii) Two vertices A1; A2 lie in one subdomain, the other two vertices A3; A4 lie in another subdomain, and the interface intersects each edge A1A3; A1A4; A2A3; A2A4 at only one point (Fig. 2.2 (left)).

(iv) The four vertices do not lie in one subdomain and the interface intersects at least one edge of K whose vertices lie in different subdomains at more than one point (Fig. 2.2 (right)).

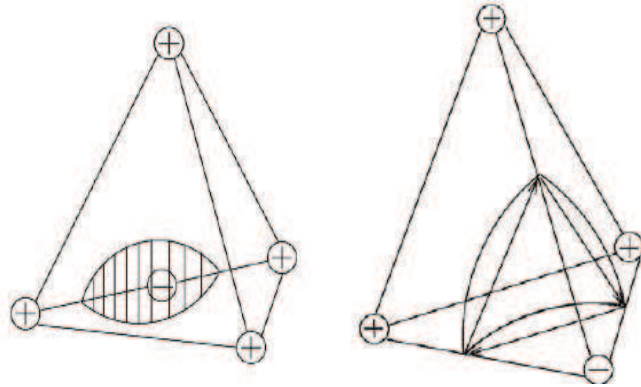


Fig. 2.1. The intersection of  $\Gamma$  with the interface element  $K$ : case (i) (left) and case (ii) (right).

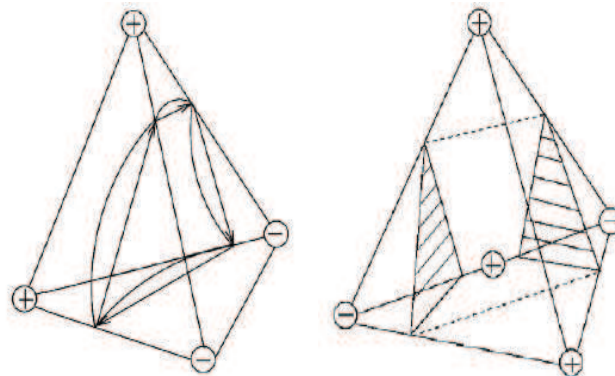


Fig. 2.2. The intersection of  $\Gamma$  with the interface element  $K$ : case (iii) (left) and case (iv) (right).

We define the discrete coefficient function  $\mu_h$  as

$$\mu_h = \begin{cases} \mu & \text{if } x \in K, \quad K \text{ non-interface element,} \\ \mu_K & \text{if } x \in K, \quad K \text{ interface element.} \end{cases} \quad (2.2)$$

For each interface element  $K \in \mathcal{M}_h^*$ ,  $\mu_K$  is defined according to the four cases as follows. In case (i) we define  $\mu_K = \mu_i$  if all four vertices lie in  $\Omega_i, i = 1, 2$ . In the cases (ii) and (iii) we first approximate the interface by plane patches connecting the intersection points between the interface and the edges of  $K$  as illustrated in Fig. 2.1 (right) and Fig. 2.2 (left). The plane patches divide  $K$  into two parts  $K_1$  and  $K_2$  so that  $K_i \subset \Omega_i$ . For each part, we set  $\mu_K = \mu_i$  if that part lies in  $\Omega_i, i = 1, 2$ . In the exceptional case (iv) as illustrated in Fig. 2.2 (right), we simply define  $\mu_K = \min_{x \in K} \mu$ . Also, we define the discrete coefficient function  $\lambda_h$  similarly.

Now to derive our discrete approximation to (2.1), we introduce an intermediate conforming mesh  $\widehat{\mathcal{M}}_h$  which is the refinement of  $\mathcal{M}_h$  by breaking each interface tetrahedron into several small tetrahedra as illustrated in Fig. 2.3 for case (ii).  $\widehat{\mathcal{M}}_h$  is then a body-fitted mesh. Let  $\widehat{V}_h$  be the  $H^1$ -conforming linear finite element space over  $\widehat{\mathcal{M}}_h$ . Set  $\widehat{V}_h^D = \widehat{V}_h \cap H_D^1(\Omega)$ . The discrete problem is then to find  $\hat{\mathbf{u}}_h \in (\widehat{V}_h^D)^3$  such that

$$(\sigma_h(\hat{\mathbf{u}}_h), \varepsilon(\mathbf{v}_h)) = (\mathbf{f}, \mathbf{v}_h) + (\mathbf{g}, \mathbf{v}_h)_{\Gamma_N} \quad \forall \mathbf{v}_h \in (\widehat{V}_h^D)^3, \tag{2.3}$$

where

$$\sigma_h(\hat{\mathbf{u}}_h) = 2\mu_h \varepsilon(\hat{\mathbf{u}}_h) + \lambda_h \text{tr}(\varepsilon(\hat{\mathbf{u}}_h)) \mathbf{I}.$$

We note that the resulting linear system (2.3) is solved on the intermediate mesh  $\widehat{\mathcal{M}}_h$ . In the following, however, the a posteriori error estimate will be performed on  $\mathcal{M}_h$ , not  $\widehat{\mathcal{M}}_h$ . Moreover,  $\mathcal{M}_h$  will be refined to produce the new mesh in the adaptive computations. As in [21], we can see that the mesh quality will not deteriorate during the adaptive iterations if the newest vertex bisection algorithm is used to refine the meshes.

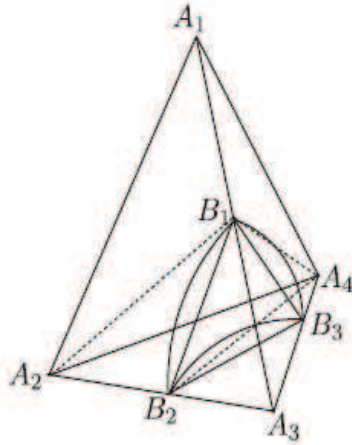


Fig. 2.3. Add new nodal points at intersections.

### 3. A Posteriori Error Analysis

A posteriori error estimates for the elasticity problems without interface have been given in some papers such as [26–29]. Among of them, [23] establishes a kind of robust a posteriori error estimate with  $\lambda$ -independent multiplicative constant. It is very important because the lamé coefficient function  $\lambda$  steers the incompressibility and the usual residual-based a posteriori estimate will lose the efficiency if  $\lambda$  is large. In this part, we will use the idea of [23] to carry out the a posteriori error analysis for our interface problems.

Now, for brevity, we define the errors

$$\mathbf{e} = \mathbf{u} - \hat{\mathbf{u}}_h, \quad \delta = \lambda \text{div}(\mathbf{u} - \hat{\mathbf{u}}_h),$$

and frequently write  $\|\cdot\|_{L^2} = \|\cdot\|_{L^2(\Omega)}$  and  $\|\cdot\|_{H^1} = \|\cdot\|_{H^1(\Omega)}$  if there is no risk of confusion.

**Lemma 3.1.** [24] *There exist a constant  $c_1(\Omega, \Gamma_N)$  and  $\mathbf{w} \in H_D^1(\Omega)^3$  function with*

$$-\operatorname{div} \mathbf{w} = \delta \quad \text{and} \quad \|\mathbf{w}\|_{H^1} \leq c_1 \|\delta\|_{L^2}. \tag{3.1}$$

Similar to [23] we employ  $\mathbf{w}$  to define functions

$$\lambda_{max} = \max(\lambda_1, \lambda_2), \quad \mu_{max} = \max(\mu_1, \mu_2), \quad \zeta = 2\mu_{max}c_1^2\mathbf{e} - \mathbf{w} \in H_D^1(\Omega)^3. \tag{3.2}$$

**Lemma 3.2.** *There exists a constant  $c_2$  depending on  $c_1$  such that*

$$\|2\mu\varepsilon(\mathbf{e})\|_{L^2}^2 + \|\delta\|_{L^2}^2 \leq c_2(2\mu\varepsilon(\mathbf{e}) + \delta I, \nabla\zeta). \tag{3.3}$$

*Proof.* A direct calculation employing the definitions above yields

$$\begin{aligned} (2\mu\varepsilon(\mathbf{e}) + \delta I, \nabla\zeta) &= (2\mu\varepsilon(\mathbf{e}) + \delta I, 2\mu_{max}c_1^2\nabla\mathbf{e} - \nabla\mathbf{w}) \\ &= (4\mu\mu_{max}c_1^2\varepsilon(\mathbf{e}), \nabla\mathbf{e}) + (\delta I, -\nabla\mathbf{w}) + (\delta I, 2\mu_{max}c_1^2\nabla\mathbf{e}) - (2\mu\varepsilon(\mathbf{e}), \nabla\mathbf{w}) \\ &\geq c_1^2\|2\mu\varepsilon(\mathbf{e})\|_{L^2}^2 + (1 + 2c_1^2\frac{\mu_{max}}{\lambda_{max}})\|\delta\|_{L^2}^2 - (2\mu\varepsilon(\mathbf{e}), \nabla\mathbf{w}). \end{aligned} \tag{3.4}$$

Employing (3.1), Cauchy’s and Young’s inequalities we deduce

$$(2\mu\varepsilon(\mathbf{e}), \nabla\mathbf{w}) \leq \frac{1}{2}c_1^2\|2\mu\varepsilon(\mathbf{e})\|_{L^2}^2 + \frac{1}{2}\|\delta\|_{L^2}^2, \tag{3.5}$$

A combination of (3.4) and (3.6) shows the assertion (3.3). □

Using lemmas above, we can prove the following a posteriori error estimate.

**Theorem 3.1.** *Let  $\mathbf{u}$  and  $\mathbf{u}_h$  be the solution of (2.1) and (2.3), respectively. There exists a constant  $C > 0$  depending on the minimum angle of  $\mathcal{M}_h$ ,  $\Omega$ ,  $c_1, c_2, \frac{\mu_{max}}{\mu_{min}}$ . Then, we have*

$$\|2\mu\varepsilon(\mathbf{e})\|_{L^2}^2 + \|\delta\|_{L^2}^2 \leq C \left( \sum_{K \in \mathcal{M}_h} \eta_K^2 \right), \tag{3.6}$$

where the local error indicator  $\eta_K$  is defined as

$$\begin{aligned} \eta_K^2 &= h_K^2 \|\mathbf{f}\|_{L^2(K)}^2 + \sum_{\hat{e} \subset K, \hat{e} \not\subset \partial\Omega} h_K \|\sigma_h(\hat{\mathbf{u}}_h)\mathbf{n}\|_{L^2(\hat{e})}^2 \\ &\quad + \sum_{\hat{e} \subset K, \hat{e} \subset \Gamma_N} h_K \|\mathbf{g} - \sigma_h(\hat{\mathbf{u}}_h)\mathbf{n}\|_{L^2(\hat{e})}^2 \\ &\quad + \beta_K \|2(\mu - \mu_h)\varepsilon(\hat{\mathbf{u}}_h) + (\lambda - \lambda_h)\operatorname{div}\hat{\mathbf{u}}_h I\|_{L^2(K)}^2. \end{aligned}$$

Here  $\beta_K = 1$  if  $K$  is an interface element, and  $\beta_K = 0$  otherwise. Moreover,  $\hat{e}$  denotes the edge of tetrahedron of partition  $\hat{\mathcal{M}}_h$ .

*Proof.* Let  $V_h$  be the piecewise linear  $H^1$ -conforming finite element space over  $\mathcal{M}_h$ . We know that there exists the Clément interpolant  $P_h : H_D^1(\Omega) \rightarrow V_h$  in [6]. For vector-valued functions,  $P_h$  is defined by applying it to the components of the function. Then, we have the following stability properties: For any element  $K$  and edge  $e$ ,

$$\|\mathbf{V} - P_h\mathbf{V}\|_{L^2(K)} \leq Ch_K \|\nabla\mathbf{V}\|_{L^2(\omega_K)}, \quad \|\mathbf{V} - P_h\mathbf{V}\|_{L^2(e)} \leq Ch_e^{\frac{1}{2}} \|\nabla\mathbf{V}\|_{L^2(\omega_e)}. \tag{3.7}$$

Moreover, we can deduce that the properties follows: For any element  $\hat{K} \in \widehat{\mathcal{M}}_h, \hat{K} \subset K$  and edge  $\hat{e} \subset \hat{K}$ ,

$$\|\mathbf{V} - P_h \mathbf{V}\|_{L^2(\hat{K})} \leq Ch_K \|\nabla \mathbf{V}\|_{L^2(\omega_K)}, \quad \|\mathbf{V} - P_h \mathbf{V}\|_{L^2(\hat{e})} \leq Ch_K^{\frac{1}{2}} \|\nabla \mathbf{V}\|_{L^2(\omega_K)}. \quad (3.8)$$

Here  $C$  depends on the minimum angle of  $\mathcal{M}_h$ .

By (2.1) and (2.3), because of Lemma 3.2 and integrating by parts, we have

$$\begin{aligned} & \|2\mu\varepsilon(\mathbf{e})\|_{L^2}^2 + \|\delta\|_{L^2}^2 \leq c_2(2\mu\varepsilon(\mathbf{e}) + \delta I, \nabla \zeta) \\ & = c_2(2\mu\varepsilon(\mathbf{u}) + \lambda \operatorname{div} \mathbf{u} I, \nabla \zeta - \nabla P_h \zeta) \\ & \quad - c_2(2\mu_h \varepsilon(\hat{\mathbf{u}}_h) + \lambda_h \operatorname{div} \hat{\mathbf{u}}_h I, \nabla \zeta - \nabla P_h \zeta) \\ & \quad - c_2 \sum_{K \in \mathcal{M}_h^*} (2(\mu - \mu_h) \varepsilon(\hat{\mathbf{u}}_h) + (\lambda - \lambda_h) \operatorname{div} \hat{\mathbf{u}}_h I, \nabla \zeta)_K \\ & = c_2 \sum_{K \in \mathcal{M}_h} \left( (\mathbf{f}, \zeta - P_h \zeta)_K + \sum_{\hat{e} \subset K, \hat{e} \notin \partial \Omega} ([\sigma_h(\hat{\mathbf{u}}_h) \mathbf{n}], \zeta - P_h \zeta)_{\hat{e}} \right. \\ & \quad \left. + \sum_{\hat{e} \subset K, \hat{e} \subset \Gamma_N} (\mathbf{g} - \sigma_h(\hat{\mathbf{u}}_h) \mathbf{n}, \zeta - P_h \zeta)_{\hat{e}} \right) \\ & \quad - c_2 \sum_{K \in \mathcal{M}_h^*} (2(\mu - \mu_h) \varepsilon(\hat{\mathbf{u}}_h) + (\lambda - \lambda_h) \operatorname{div} \hat{\mathbf{u}}_h I, \nabla \zeta)_K. \end{aligned} \quad (3.9)$$

By (3.8) and a few applications of Cauchy’s inequality we can have

$$\|2\mu\varepsilon(\mathbf{e})\|_{L^2}^2 + \|\delta\|_{L^2}^2 \leq C(c_2, \mathcal{M}_h) \left( \sum_{K \in \mathcal{M}_h} \eta_K^2 \right)^{\frac{1}{2}} \|\nabla \zeta\|_{L^2}.$$

By Korn’s inequality, the definition of  $\zeta$  and Lemma 3.1, we obtain

$$\|\nabla \zeta\|_{L^2} \leq C(\Omega, c_1, \frac{\mu_{max}}{\mu_{min}}) \left( \|2\mu\varepsilon(\mathbf{e})\|_{L^2} + \|\delta\|_{L^2} \right). \quad (3.10)$$

Thus, using Young’s inequality, we can get the assertion of (3.6). □

### 4. Adaptive Algorithm and Numerical Experiments

The implementation of our 3D AIIFEM method is based on the parallel adaptive finite element package PHG [15, 16]. The computation is carried out on O3800 in the State Key Laboratory on Scientific and Engineering Computing of Chinese Academy of Sciences.

**Algorithm 4.1.**  
 Given tolerance  $TOL > 0$ .

- Generate an initial mesh  $\mathcal{M}_0, k = 0$ ;
- While  $\mathcal{E}_k = \left( \sum_{K \in \mathcal{M}_k} \eta_K^2 \right) > TOL$ , do
  - Designate the discrete coefficient functions  $\mu_K, \lambda_K$  on  $\mathcal{M}_k$ ;
  - add new elements in interface elements to generate intermediate conforming mesh  $\widehat{\mathcal{M}}_k$ ;
  - Solve the discrete problem on  $\widehat{\mathcal{M}}_k$ ;
  - Compute the local error indicator  $\eta_K$  on each  $K \in \mathcal{M}_k$ ;
  - Refine all  $K \in \mathcal{M}_k$  satisfying  $\eta_K > \frac{1}{2} \max_{K \in \mathcal{M}_k} \eta_K$  to construct conforming mesh  $\mathcal{M}_{k+1}$ ;
  - Set  $k = k + 1$ .
- End while

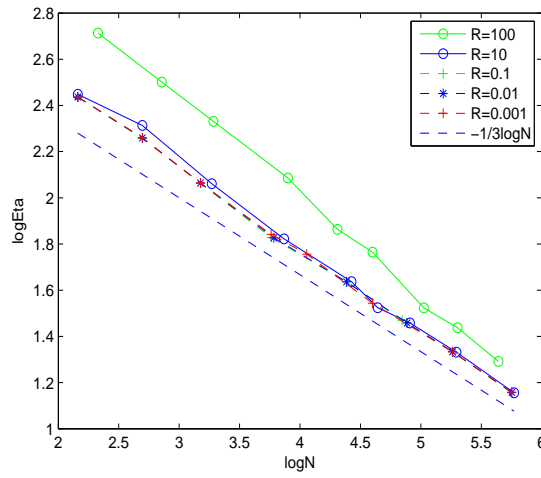


Fig. 4.1. The quasi-optimal convergence of the a posteriori error estimates (Example 4.1).

Now we report several numerical experiments to demonstrate the competitive behavior of the algorithm. The discrete system of linear equations is solved by preconditioned CG method.

**Example 4.1.** Let  $\Omega = (-2, 2)^3$  and the interface be a unit sphere centered at the origin. The exact solution is given in the spherical coordinates as

$$u_1(r) = u_2(r) = u_3(r) = \begin{cases} (r^2 - 1)/R + 1 & \text{if } r \leq 1; \\ r^2 & \text{if } r > 1. \end{cases} \quad (4.1)$$

We set the  $\lambda(x) = \mu(x) = R$  inside the sphere and  $\lambda(x) = \mu(x) = 1$  outside.

Fig. 4.1 shows the  $\log\mathcal{E}$ - $\log N$  curves for different values of  $R$ , where  $\mathcal{E}$  is the a posteriori error estimate and  $N$  is the number of degrees of freedom. It indicates that the adaptive

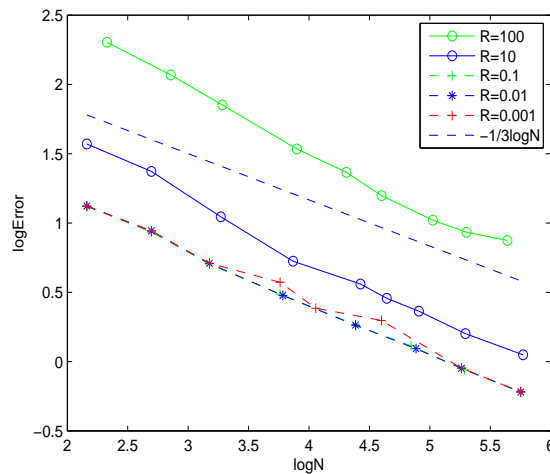


Fig. 4.2. The quasi-optimal convergence of the error (Example 4.1).

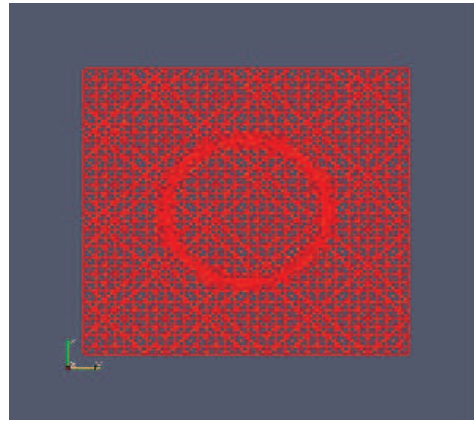


Fig. 4.3. A slice of adaptively refined mesh at  $x_1 = 0$  (Example 4.1).

meshes and the associated computational complexity are quasi-optimal:  $\mathcal{E} = CN^{-1/3}$  is valid asymptotically. Fig. 4.2 shows the  $\log \mathcal{E}_{rr} - \log N$  curves for different values of  $R$ , where  $\mathcal{E}_{rr}$  is the error in the norm defined above. Fig. 4.3 shows an adaptive mesh using 94099 degrees of freedom when  $R = 100$ .

**Example 4.2.** Let  $\Omega = (-2, 2)^3$  and the interface be a unit sphere centered at the origin. The exact solution is the same as the one given in Example 1. But here we set the  $\lambda(x) = 50 \times R, \mu(x) = R$  inside the sphere and  $\lambda(x) = 50, \mu(x) = 1$  outside.

Fig. 4.4 shows the  $\log \mathcal{E} - \log N$  curves for different values of  $R$ , where  $\mathcal{E}$  is the a posteriori error estimate and  $N$  is the number of degrees of freedom. It indicates that the adaptive meshes and the associated computational complexity are quasi-optimal:  $\mathcal{E} = CN^{-1/3}$  is valid asymptotically. Fig. 4.5 shows the  $\log \mathcal{E}_{rr} - \log N$  curves for different values of  $R$ , where  $\mathcal{E}_{rr}$  is the error in the norm defined above. Fig. 4.6 shows an adaptive mesh using 232999 degrees of freedom when  $R = 10$ .

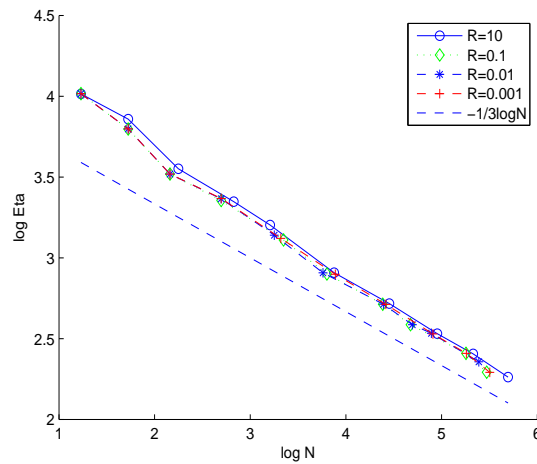


Fig. 4.4. The quasi-optimal convergence of the a posteriori error estimates (Example 4.2).

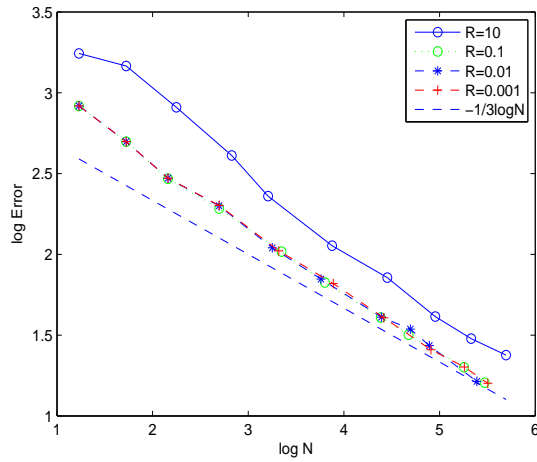


Fig. 4.5. The quasi-optimal convergence of the error (Example 4.2).

**Example 4.3.** Let  $\Omega = (-2, 2)^3$  and the interface be a unit sphere centered at the origin. Let  $\mathbf{f} = 0$  The boundary condition is given as

$$\begin{aligned}
 u_1|_{\partial\Omega} &= u_2|_{\partial\Omega} = u_3|_{\partial\Omega} \\
 &= \sin((x + 2) * (y + 2) * (z + 2)) + (x + 2) * (y + 2) * (z + 2). \tag{4.2}
 \end{aligned}$$

We set the  $\lambda(x) = 40 \times R, \mu(x) = 10 \times R$  inside the sphere and  $\lambda(x) = 25, \mu(x) = 10$  outside.

Fig. 4.7 shows the  $\log\mathcal{E}$ - $\log N$  curves for different values of  $R$ , where  $\mathcal{E}$  is the a posteriori error estimate and  $N$  is the number of degrees of freedom. It indicates that the adaptive meshes and the associated computational complexity are quasi-optimal:  $\mathcal{E} = CN^{-1/3}$  is valid asymptotically. Fig. 4.8 shows an adaptive mesh using 217239 degrees of freedom when  $R = 100$ .

**Example 4.4.** In this example we consider an problem involving an interface having cusps see Fig. 4.9. We set the computational domain  $\Omega = (-2, 2)^3, \Omega_1 = \{\mathbf{x} = (x_1, x_2, x_3), x_1 > 0, x_2 >$

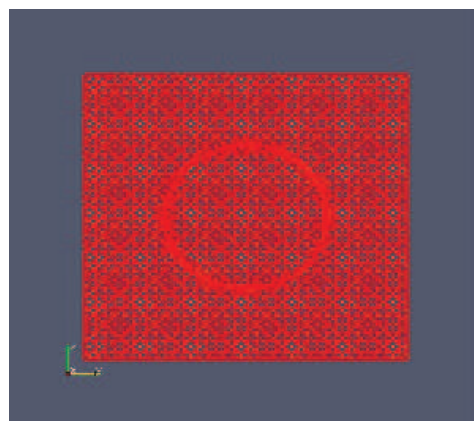


Fig. 4.6. A slice of adaptively refined mesh at  $x_1 = 0$  (Example 4.2).

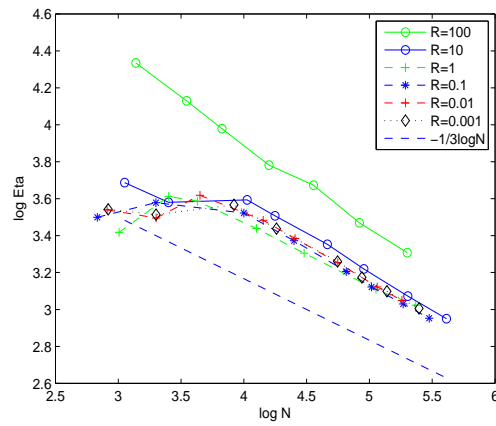


Fig. 4.7. The quasi-optimal convergence of the a posteriori error estimates (Example 4.3).

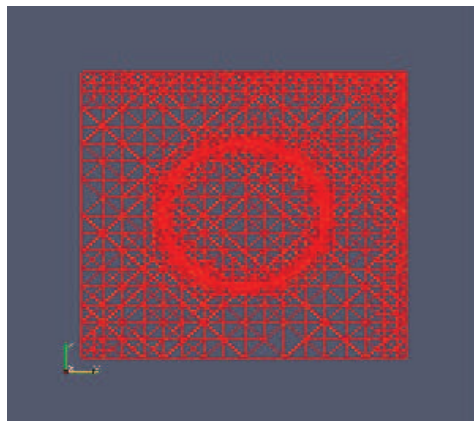


Fig. 4.8. A slice of adaptively refined mesh at  $x_1 = 0$  (Example 4.3).

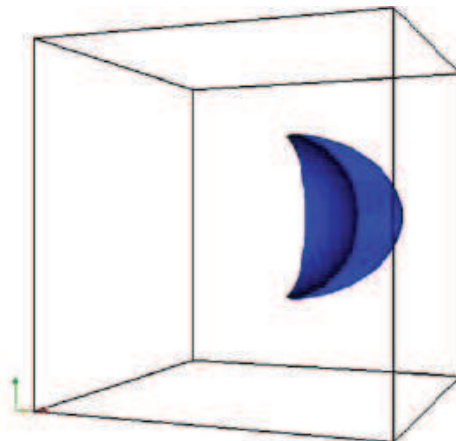


Fig. 4.9. The configuration of the interface used in Example 4.4.

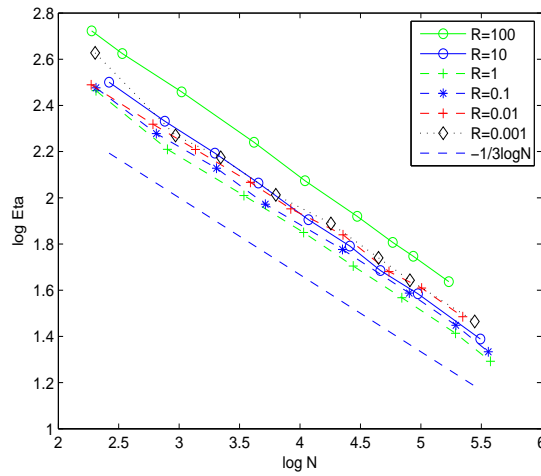


Fig. 4.10. The quasi-optimal convergence of the a posteriori error estimates (Example 4.4).

$0, \mathbf{x} \in S_1 \setminus S_2\}$ , where  $S_1$  and  $S_2$  are defined by:

$$S_1 : \frac{x_1^2}{1.5^2} + \frac{x_2^2}{1.5^2} + x_3^2 < 1, \tag{4.3}$$

$$S_2 : x_1^2 + x_2^2 + x_3^2 \leq 1. \tag{4.4}$$

Note that the interface  $\Gamma$  is not even Lipschitz continuous and has the singularity at the cusp points  $(0, 0, \pm 1)$ . We set the  $\lambda(x) = 40 \times R, \mu(x) = 10 \times R$  in  $\Omega_1$  and  $\lambda(x) = 25, \mu(x) = 10$  outside. Moreover,  $\mathbf{f} = -10$  in  $\Omega$ , and  $\mathbf{u} = 0$  on the boundary.

Fig. 4.10 shows the  $\log \mathcal{E}$ - $\log N$  curves for different values of  $R$ , where  $\mathcal{E}$  is the a posteriori error estimate and  $N$  is the number of degrees of freedom. It indicates that the adaptive meshes and the associated computational complexity are quasi-optimal:  $\mathcal{E} = CN^{-1/3}$  is valid asymptotically. Fig. 4.11 shows an adaptive mesh using 215009 degrees of freedom when  $R = 0.1$ .

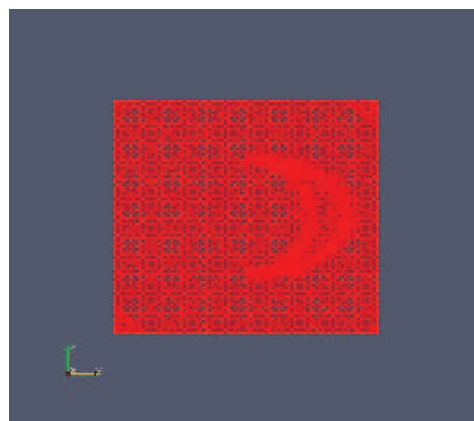


Fig. 4.11. A slice of adaptively refined mesh at  $x_1 = 0$  (Example 4.4).

## 5. Concluding Remarks

In this paper we develop the adaptive immersed interface finite element method for solving the elasticity interface problems. The finite element meshes are adaptively refined according to local a posteriori error estimators which are  $\lambda$ -independent multiplicative constants and need not fit with the interfaces. Our extensive numerical experiments indicate that the proposed algorithm can handle geometrically complicated interfaces that may have tips or cusps so that the exact solution of the problems may have strong singularities. For the nearly incompressible case ( $\lambda$  approaches infinity), we will extend the adaptive methods to solve it.

**Acknowledgments.** This paper is supported in part by China NSF under the grant 11101025 and by the Fundamental Research Funds for the Central Universities.

## References

- [1] R.J. Asaro and W.A. Tiller, Surface morphology development during stress corrosion cracking: Part I: via surface diffusion, *Metall. Trans.*, **3** (1972), 1789-1796.
- [2] M.A. Grinfeld, The stress driven rearrangement instability in elastic crystals: mathematical models and physical manifestations, *J. Nonlinear Sci.*, **3** (1993), 35-83.
- [3] H. Jou, H. Leo and J.S. Lowengrub, Microstructural evolution in inhomogeneous elastic media, *J. Comp. Phys.*, **131**:1 (1997), 109-148.
- [4] I. Babuška, The finite element method for elliptic equations with discontinuous coefficients, *Computing*, **5** (1970), 207-213.
- [5] Z. Chen and J. Zou, Finite element methods and their convergence for elliptic and parabolic interface problems, *Numer. Math.*, **79** (1998), 175-202.
- [6] P. Clément, Approximation by finite element functions using local regularization, *RAIRO Anal. Numer.*, **9** (1975), 77-84.
- [7] R. LeVeque and Z. Li, The immersed interface method for elliptic equations with discontinuous coefficients and singular sources, *SIAM J. Numer. Anal.*, **31** (1994), 1019-1044.
- [8] Z. Li, K. Ito, *The Immersed Interface Method: Numerical Solutions of PDEs Involving Interfaces and Irregular Domains*, SIAM (2006).
- [9] Z. Li, T. Lin and X. Wu, New Cartesian grid methods for interface problems using the finite element formulation, *Numer. Math.*, **96** (2003), 61-98.
- [10] Z. Li and P. Song, An adaptive mesh refinement strategy for immersed boundary/interface methods, *Commun. Comput. Phys.*, **12** (2012), 515-527.
- [11] S. Hou, Z. Li, L. Wang and W. Wang, A numerical method for solving elasticity equations with interfaces, *Commun. Comput. Phys.*, **12** (2012), 595-612.
- [12] Y. Gong and Z. Li, Immersed interface finite element methods for elasticity interface problems with non-homogeneous jump conditions, *Numer. Math. Theor. Meth. Appl.*, **3** (2010), 23-39.
- [13] X. Liu, R.P. Fedkiw and M. Kang, A boundary condition capturing method for Poissons equation on irregular domains, *J. Comp. Phys.*, **160** (2000), 151-178.
- [14] C.S. Peskin, Numerical analysis of blood flow in heart, *J. Comp. Phys.*, **25** (1977), 220-252.
- [15] L. Zhang, PHG: Parallel Hierarchical Grid, State Key Laboratory of Scientific and Engineering Computing of Chinese Academy of Sciences, 2007, <<http://lsec.cc.ac.cn/phg/>>.
- [16] L. Zhang, A parallel algorithm for adaptive local refinement of tetrahedral meshes using bisection, *Numer. Math. Theor. Meth. Appl.*, **2** (2009), 65-89.
- [17] X. Yang, *Immersed Interface Method for Elasticity Problems with Interfaces*, North Carolina State University, 2004.
- [18] X. Yang, B. Li and Z. Li, The immersed interface method for elasticity problems with interface, *Dyn. Contin. Discrete Impuls. Syst. Ser. A Math. Anal.*, **10**:5 (2003), 783-808.

- [19] Y. Gong, Immersed Interface Finite Element Methods for Elliptic and Elasticity Interface Problems, North Carolina State University, 2007.
- [20] Y. Gong and Z. Li., Immersed interface finite element methods for elasticity interface problems with nonhomogeneous jump conditions, *Numer. Math. Theor. Meth. Appl.*, **3** (2010), 23-39.
- [21] Z. Chen, Y. Xiao and L. Zhang, The adaptive immersed interface finite element method for elliptic and Maxwell interface problems, *J. Comp. Phys.*, (2009), doi:10.1016/j.jcp.2009.03.044.
- [22] H. Wu, High order scheme for schrodinger equation with discontinuous potential I: immersed interface method, *Numer. Math. Theor. Meth. Appl.*, **4** (2011), 576-597.
- [23] C. Carstensen and S.A. Funken, Averaging technique for FE - a posteriori error control in elasticity. Part II:  $\lambda$ -independent estimates, *Comput. Methods Appl. Mech. Engrg.*, **109** (2001), 4663-4675.
- [24] F. Brezzi and M. Fortin, Mixed and Hybrid Finite Element Methods, Springer, Berlin, 1991.
- [25] J.L. Lions, Optimal Control of Systems Governed by Partial Differential Equations, Springer-Verlag, Berlin, 1971.
- [26] R. Verfürth, A Review of A Posteriori Error Estimation and Adaptive Mesh-Refinement Techniques, Wiley-Teubner, Stuttgart, 1996.
- [27] R. Verfürth, A Review of A Posteriori Error Estimation Techniques for Elasticity Problems, On New Advances in Adaptive Computational Methods in Mechanics, Elsevier, 1997.
- [28] F. Cirak and E. Ramm, A posteriori error estimation and adaptivity for linear elasticity using the reciprocal theorem, *Comput. Methods Appl. Mech. Engrg.*, **156** (1998), 352-362.
- [29] M. Rüter and E. Stein, Goal-oriented a posteriori error estimates in linear elastic fracture mechanics, *Comput. Methods Appl. Mech. Engrg.*, **195** (2006), 251-278.